This article has an erratum available at: https://dx.doi.org/10.21037/cdt-2023-2 and the article has been update on 2023-03-30 at here.

Original Article

Feasibility of 3.0 T balanced fast field echo non-contrast-enhanced whole-heart coronary magnetic resonance angiography

Yang Chen[1,2#], Hao Guo[2#], Peng Dong[1#], Yue Li[2], Zhongsheng Zhang[2], Ning Mao[2], Tongpeng Chu[2], Zehua Sun[2], Fang Wang[2], Zhiqiang Feng[2], Huaying Wang[2], Heng Ma[2]

[1]Department of Medical Imaging, Weifang Medical University, Weifang, China; [2]Department of Radiology, Qingdao University and Yantai Yuhuangding Hospital, Yantai, China

Contributions: (I) Conception and design: All authors; (II) Administrative support: H Ma, P Dong; (III) Provision of study materials or patients: All authors; (IV) Collection and assembly of data: Y Chen, H Guo; (V) Data analysis and interpretation: All authors; (VI) Manuscript writing: All authors; (VII) Final approval of manuscript: All authors.

[#]These authors contributed equally to this work.

Correspondence to: Heng Ma. Department of Radiology, Qingdao University and Yantai Yuhuangding Hospital, Yuhuangding East Road 20, Zhifu, Yantai, China. Email: mhyhdyy@163.com.

Background: Coronary artery disease (CAD) is one of the most common diseases seriously harmful to human health caused by atherosclerosis. Besides coronary computed tomography angiography (CCTA) and invasive coronary angiography (ICA), coronary magnetic resonance angiography (CMRA) has become an alternative examination. The purpose of this study was to prospectively evaluate the feasibility of 3.0 T free-breathing whole-heart non-contrast-enhanced coronary magnetic resonance angiography (NCE-CMRA).

Methods: After Institutional Review Board approval, the NCE-CMRA data sets of 29 patients acquired successfully at 3.0 T were evaluated independently by two blinded readers for visualization and image quality of coronary arteries using the subjective quality grade. The acquisition times were recorded in the meantime. A part of the patients had undergone CCTA, we represented stenosis by scores and used the Kappa to evaluate the consistency between CCTA and NCE-CMRA.

Results: Six patients did not get diagnostic image quality because of severe artifacts. The image quality score assessed by both radiologists is 3.2±0.7, which means the NCE-CMRA can show the coronary arteries excellently. The main vessels of the coronary artery on NCE-CMRA images are considered reliably assessable. The acquisition time of NCE-CMRA, is 8.8±1.2 min. The Kappa of CCTA and NCE-CMRA on detecting stenosis is 0.842 (P<0.001).

Conclusions: The NCE-CMRA results in reliable image quality and visualization parameters of coronary arteries within a short scan time. The NCE-CMRA and CCTA have a good agreement for detecting stenosis.

Keywords: Coronary artery disease (CAD); magnetic resonance angiography; image quality; non-contrast-enhanced (NCE); computed tomography angiography

Submitted Sep 21, 2022. Accepted for publication Dec 02, 2022. Published online Dec 29, 2022.
doi: 10.21037/cdt-22-487
View this article at: https://dx.doi.org/10.21037/cdt-22-487

Introduction

Coronary artery disease (CAD) is one of the leading causes of death in middle-aged and older adults. With the development of the economy and the improvement of living standard in various countries around the world, the incidence of coronary atherosclerotic heart disease is increasing and becoming younger (1). Coronary artery stenosis is an important basis for imaging diagnosis of coronary heart disease. The gold criteria examination for detecting coronary stenosis is conventional X-ray coronary

angiography (2). However, it is limited for screening CAD due to its invasiveness and costs. Coronary computed tomography angiography (CCTA) has disadvantages such as radiation and invasiveness, which may limit its use in some people because of the risk of allergic reactions caused by contrast agents, although it is the most common method for the diagnosis of CAD (1,3,4). Magnetic resonance imaging (MRI) is a promising non-invasive and non-radiative examination for assessing the coronary arteries, so the non-contrast-enhanced coronary magnetic resonance angiography (NCE-CMRA) is expected to detect coronary stenosis though its precise visualization remains a challenge compared with CCTA (5).

By applying the 3D free-breathing method to whole-heart coronary magnetic resonance angiography (CMRA), several studies have attempted to improve the assessment of coronary artery stenosis and provide an accurate diagnosis of clinically significant lesions (6). Previous studies had confirmed that both 1.5 T NCE-CMRA and 3.0 T contrast-enhanced coronary magnetic resonance (CE-CMRA) can detect coronary artery stenosis (7-9). 1.5 T NCE-CMRA has a lower signal-to-noise ratio (SNR) and resolution compared with 3.0 T CMRA (7,10). The 3.0 T NCE-CMRA needs the Gadolinium contrast agent (11). Therefore, we aimed to get high SNR and resolution without the agent. The contrast weight of the conventional sequence is T_1 or T_2, however, the balanced turbo-field-echo (B-TFE) sequence use T_2/T_1 as contrast weight which can highlight blood signal brightness by combined with the fat suppression technique (12). Therefore, the objective of this study was to verify the feasibility of the free-breathing whole-heart NCE-CMRA at 3.0 T using the B-TFE sequence and its consistency with CCTA for detecting stenosis.

Highlight box

Key findings

- The 3.0 T non-contrast-enhanced coronary magnetic resonance angiography using balanced turbo-field-echo sequence can get good image quality, visualization, short acquisition time, and consistency of detecting stenosis with coronary computed tomography angiography.

What is known and what is new?

- The 3.0 T non-contrast-enhanced magnetic resonance angiography can be used to assessment the coronary artery.
- We demonstrated the feasibility of 3.0 T non-contrast-enhanced magnetic resonance angiography using balanced turbo-field-echo sequence at to observe the coronary artery.

What is the implication, and what should change now?

- The 3.0 T non-contrast-enhanced coronary magnetic resonance angiography using balanced turbo-field-echo sequence may become an optional clinical examination to observe the coronary artery in the future. The better technique or sequence should be used to improve the image quality, visualization, and reduce the acquisition time.

Methods

Study population

Thirty-five patients underwent NCE-CMRA from January 2021 to March 2022, of whom 29 had previously undergone CCTA. Besides, there are 9 patients who did not perform the scanning successfully. We recruited 44 patients from Yantai Yuhuangding hospital randomly in total. The study was conducted in accordance with the Declaration of Helsinki (as revised in 2013). This research was approved by the Ethics Committee of Yantai Yuhuangding Hospital (No. 2021-453). All patients signed informed consent forms. The exclusion criteria were heart rates >75 bpm, orthopnea, history of previous cardiac surgery or coronary revascularization, presence of coronary artery stent, contraindications to MRI (pacemaker, claustrophobia), thyroid disorder, and impaired renal function (creatinine >1.4 mg/dL). *Table 1* shows the characteristics of all patients.

Patients rested for 5 minutes after arriving in the MRI waiting area to prevent rapid heart rate due to exercise before NCE-CMRA. In addition, 0.5 mg nitroglycerin was prepared in case of a cardiovascular incident. To reduce abdominal motion during deep inspiration, a medical abdominal belt was wrapped tightly along the side of the ribs. No patient was taken nitroglycerin or β-blocker before the NCE-CMRA scan.

NCE-CMRA scan

NCE-CMRA was performed by a 3.0 T system (PHILIP INGENIA; Philips Healthcare, Erlangen) equipped with the 32-channel dStream Torso coil covering the entire heart. The scan protocol includes retrospective electrocardiography (ECG)-triggered cine sequence and two-dimensional single-shot B-TFE sequence. An abdominal band was used to reduce the effect of respiratory motion artifacts during scanning. We triggered the data acquisition by the R-wave acquired from a three-

Table 1 Characteristics of study population

Number	Number (n=29)
Age (y)	54±15.5
Height (cm)	165.7±8.2
Weight (kg)	67.2±10.6
BMI (kg/m^2)	24.5±3.3
Sex (male/female)	16/13
Smoking, n (%)	8 (27.6)
Hypertension, n (%)	11 (37.9)
Dyslipidemia, n (%)	10 (34.5)
Diabetes mellitus, n (%)	2 (6.9)
Ischemia/non-ischemia	15/14

The data were presented as the mean ± standard deviation or as the number (%) of subjects. BMI, body mass index.

Table 2 Parameters gotten during the scanning

Parameter	Value
Shot duration (msec)	88.3±13.1
Average gating efficiency (%)	57.3±23.8
Heart rate (bmp)	63.5±5.9

Numbers are mean values ± standard deviations for 29 patients.

lead wireless vector cardiogram. The NCE-CMRA scanning location was performed in left ventricular short axis, 2-chamber, and 4-chamber heart plane views. The retrospective ECG-triggered cine sequence was performed in the 4-chamber heart plane to determine the quiescent period window by the minimal motion of the right coronary artery (RCA) (13). The visual evaluation was used to determine the trigger delay time and acquisition duration of every patient, freezing respiratory movement by using diaphragmatic navigation. Place the navigation bar on the right diaphragm with lung tissue in the upper 1/3 and liver tissue in the lower 2/3. For whole-heart NCE-CMRA, an ECG-triggered, prospective diaphragm navigator-gated, B-TFE sequence was employed. The scanning was performed using the following parameters: 2.0/4.0 (echo time msec/repetition time msec), a 12° flip angle, 300×252×128 (field of view mm), a reconstruction matrix of 232×179×160, an acquired voxel size of 1.3×1.4×1.6 mm, a reconstruction voxel size of 0.62×0.62×0.80 mm, a scale factor of 0.6, and a gating window of 4. *Table 2* summarized the parameters which were gotten during the scanning. *Figure 1* shows the original axial images of NCE-CMRA.

NCE-CMRA images were transferred to the Philips workstation (IntelliSpace Portal, Philips Healthcare, Netherlands) and reconstructed at the end of the acquisition on the workstation. The senior radiologist blinded to original images processed curved planar reconstruction (CPR) of left circumflex (LCX), left anterior descending (LAD), and RCA of axial images, and then measured the length of the vessels using the workstation. One representative image of the NCE-CMRA is shown in *Figure 2*. The volume reconstruction (VR) images of NCE-CMRA were processed by the cardiac MR analysis tool. The representative VR images are shown in *Figure 3*.

Qualitative image quality and visual analysis

Two senior radiologists with cardiovascular MRI experience independently evaluated image quality for each segment based on a 4-point scale according to the border definition and artifact of vessels, as follows: 4= excellent (no artifact and sharply defined); 3= good (slight artifact and mildly blurred); 2= fair (moderate artifact and markedly blurred); 1= poor (severe artifact and nondiagnostic). Only segments with the score of 3 or 4 assessed by two radiologists consistently were included in the final stenosis assessment compared with CCTA. We incorporated 8 coronary segments into the analysis refer to the classification of the American Heart Association (14), as follows: (segment 1) RCA proximal, (segment 2) RCA middle, (segment 3) RCA distal, (segment 6) LAD proximal, (segment 7) LAD middle, (segment 8) LAD distal, (segment 11) LCX proximal, and (segment 13) LCX distal. The third radiologist evaluated the image quality when two observers assessed differently in the axial orientation. Radiologist 1 assessed the image quality, and we computed the inter-observer agreement with radiologist 2 for subsequent analysis.

Quantitative visual analysis of vessel

The parameters included visible vessel length, diameter, and sharpness. The diameter and sharpness of the vessels were evaluated in segments 1, 6, and 11. The vessel diameter was computed as the full width at half between background and maximum (15). To assess the sharpness of the vessel, the 80% and 20% points between the background signal and maximal intensities were computed for each side of the signal intensity profile at first. The vessel sharpness

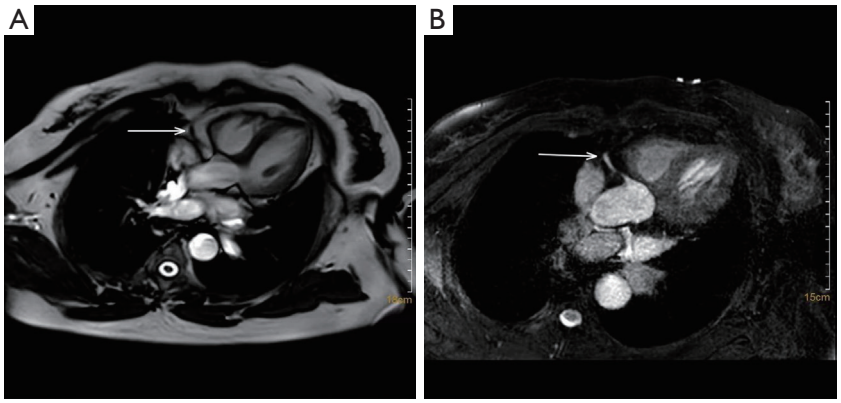

Figure 1 The cine sequence and B-TFE sequence of whole-heart free-breathing NCE-CMRA at 3.0 T from a 70-year-old woman. (A) The axial image of NCE-CMRA scanned by cine sequence. The arrow points to the RCA. (B) The axial image of NCE-CMRA scanned by B-TFE sequence. The arrow points to the RCA. B-TFE, balanced turbo-field-echo; NCE-CMRA, non-contrast-enhanced coronary magnetic resonance angiography; RCA, right coronary artery.

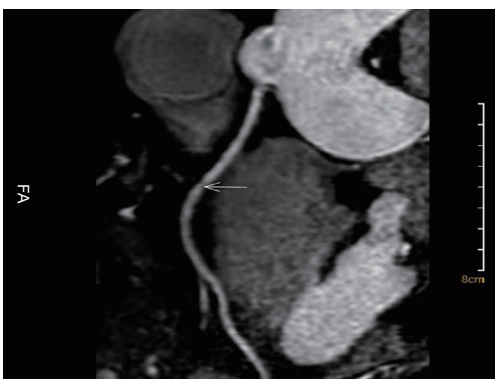

Figure 2 The CPR of 3.0 T whole-heart free-breathing NCE-CMRA based on B-TFE sequence from a 40-year-old man. The arrow points to the LAD. CPR, curve planar reformation; NCE-CMRA, non-contrast-enhanced coronary magnetic resonance angiography; B-TFE, balanced turbo-field-echo; LAD, left anterior descending; FA, feet anterior.

was defined as the inverse of the averaged distance in millimeters determined for each side between the two points (16).

Evaluation of consistency between CCTA and NCE-CMRA for detecting stenosis

We did not apply invasive coronary angiography (ICA) as the standard examination because of slight clinical symptoms, high expense, and stent implantation. The stenosis of each segment in both examinations were counted as scores in all patients (2= significant stenosis; 1= mild stenosis; 0= no stenosis). The significant stenosis performed as stenosis >50% (17).

Statistical analysis

In all statistical analyses using SPSS version 26.0 (SPSS Inc., Chicago, Illinois, USA), the quadratic-weighted Kappa test was used to evaluate the consistency of NCE-CMRA and dual source coronary computed tomography angiography (DS-CCTA) for detecting stenosis. The Kappa coefficient <0.4 indicates poor agreement, and ≥0.75 indicates good agreement.

Results

These patients underwent B-TFE NCE-CMRA, the respiratory acceptance rate and acquisition time are shown in *Table 2*, and no segment was excluded from the image quality and visualization analysis. The acquisition time of the NCE-CMRA is 8.8±1.2 min. Except for these patients, 2 patients were excluded for sudden discomfort before the NCE-CMRA scan, 7 patients canceled the examination after signing the informed consent. In total, 87 vessels and 232 coronary artery segments from 29 patients were evaluated. The image quality score assessed by both radiologists is 3.2±0.7. There are 210 (90.5%) and 209 (90.1%) segments of 232 segments with the score of 3 or 4 assessed by radiologist 1 and radiologist 2. This means the images we obtained can be used to observe the anatomical

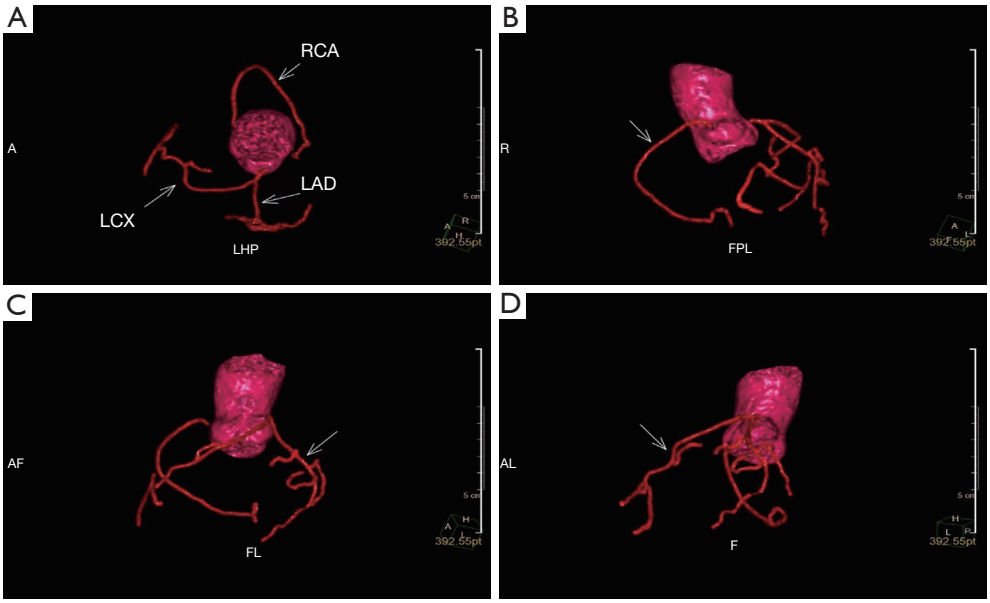

Figure 3 The VR of 3.0 T whole-heart free-breathing NCE-CMRA based on B-TFE sequence from a 47-year-old woman. (A) The axial image of RCA, LAD, and LCX. (B) The arrow points to the RCA. (C) The arrow points to the LAD. (D) The arrow points to the LCX. VR, volume reconstruction; NCE-CMRA, non-contrast-enhanced coronary magnetic resonance angiography; B-TFE, balanced turbo-field-echo; RCA, right coronary artery; LAD, left anterior descending; LCX, left circumflex; LHP, left head posterior; FPL, feet posterior left; AF, anterior feet; FL, feet left; AL, anterior left; A, anterior; R, right; H, head; F, feet; L, left; P, posterior; pt, point.

details of the major branches of the coronary arteries. *Table 3* summarizes the image quality scores of each coronary artery segment. The two radiologists make good agreement in subjective image quality scores (Kappa =0.82, P<0.001). The data demonstrated that the image quality of proximal segments was higher than distal segments. *Table 4* shows the visual parameters of each vessel. The length, diameter, and sharpness of RCA are apparently higher than the other two vessels.

Twenty-three patients underwent CCTA, 21 (11.4%) segments have significant stenosis, and 43 (23.4%) segments have mild stenosis. Twenty-four segments were excluded because the image quality score of NCE-CMRA <3, 160 segments were evaluated for stenosis at last. *Table 5* shows the stenosis scores of two examinations. For NCE-CMRA, 21 (13.1%) segments had significant stenosis, and 34 (21.2%) segments have mild stenosis. For CCTA, 20 (12.5%) segments have significant stenosis, and 38 (23.8%) segments had mild stenosis. *Table 5* summarizes the stenosis scores of each segment in NCE-CMRA and CCTA. Representative images of coronary stenosis detected by NCE-CMRA and CCTA are shown in *Figure 4*. Overall, there is good agreement between NCE-CMRA and CCTA in the detection of stenosis (Kappa coefficient =0.84, P<0.001).

Discussion

From this single-center, prospective study, we made the first report on the feasibility of free-breathing 3.0 T whole-heart B-TFE NCE-CMRA and its consistency with CCTA for detecting stenosis in a clinical protocol. NCE-CMRA enabled an acceptable shorter acquisition time with good image quality. Our study included some cases of obesity and obtained good image quality, which may be affected by excess fat. We used the abdominal belt technique to suppress the breathing-related motion of the diaphragm, which improved image quality and shortened acquisition time during all examinations (18). Besides, this study not only counted significant stenosis but also included segments with stenosis ≤50%, so our analysis covered all degrees of stenosis.

The visual parameters of 3.0 T NCE-CMRA were better than 1.5 T NCE-CMRA, this was probably because of the higher SNR and resolution (19). There were some differences between our data and 3.0 T NCE-CMRA although the two examinations had generally similar results,

Table 3 Radiologist assessment of image quality for segments of coronary arteries

Segment	Image quality scores							
	Radiologist 1				Radiologist 2			
	1	2	3	4	1	2	3	4
RCA proximal	0	1	7	21	0	1	5	23
RCA middle	1	1	11	16	0	2	13	14
RCA distal	2	0	17	10	0	2	18	9
LAD proximal	1	0	8	20	0	1	19	9
LAD middle	0	2	15	12	0	2	16	11
LAD distal	2	3	22	2	1	3	23	2
LCX proximal	0	2	13	14	0	3	12	14
LCX distal	3	4	20	2	4	4	19	2

Data are numbers of segments, in a total of 29 patients. Image quality for each segment based on a 4-point scale according to the border definition and artifact of vessels, as follows: 4= excellent (no artifact and sharply defined); 3= good (slight artifact and mildly blurred); 2= fair (moderate artifact and markedly blurred); 1= poor (severe artifact and nondiagnostic). RCA, right coronary artery; LAD, left anterior descending; LCX, left circumflex.

Table 4 Visual measurement

Variables	Length (mm)	Diameter (mm)	Sharpness (1/mm)
RCA	148.8±7.9	4.0±0.6	0.94±0.03
LAD	129.8±12.0	3.7±0.5	0.92±0.03
LCX	90.7±8.1	3.2±0.6	0.88±0.03

The data were presented as the mean ± standard deviation. RCA, right coronary artery; LAD, left anterior descending; LCX, left circumflex.

we thought the main reasons were different sequences and whether nitroglycerin was used before the scan (20,21). For the stenosis score of each segment, we thought the artifact caused by calcification on CCTA could make difference between the two examinations.

NCE-CMRA does not require the use of contrast agent, so it can be applied to special groups such as pregnant women and patients with renal insufficiency (1). Another advantage is that it is compatible with film acquisition which provides a smaller amplitude of motion of coronary arteries (22). In addition, the characteristics of multi-sequence and multi-parameter scanning can make MRI

Table 5 Radiologist assessment of NCE-CMRA compared with CCTA for detection of significant stenosis in 160 segments

Segment	Stenosis score					
	NCE-CMRA			CCTA		
	0	1	2	0	1	2
RCA proximal	11	8	3	11	8	3
RCA middle	14	4	3	14	5	2
RCA distal	16	4	1	15	5	1
LAD proximal	9	7	6	9	6	7
LAD middle	12	5	4	13	5	3
LAD distal	17	0	1	17	0	1
LCX proximal	13	5	2	11	7	2
LCX distal	13	1	1	12	2	1

Data are stenosis scores of 160 segments. 2= significant stenosis; 1= mild stenosis; 0= no stenosis. NCE-CMRA, non-contrast-enhanced coronary magnetic resonance angiography; CCTA, coronary computed tomography angiography; RCA, right coronary artery; LAD, left anterior descending; LCX, left circumflex.

be combined with functional imaging (23). Moreover, 9 patients have an intramural coronary artery which was detected by NCE-CMRA.

The NCE-CMRA scan and subsequent lumen stenosis assessment were time-consuming and labor-intensive processes and the acquisition time of most of the studies was not short enough. Still, there are techniques that might make our results even better, and we think it is likely that those techniques will be used in the future studies. For improving image quality, the modified Dixon fat suppression technique enables obtaining a better fat suppression effect, simultaneously overcomes the susceptibility artifact of the B-TFE sequence and makes up for the deficiency of 3.0 T bright blood (10,12). The 5D whole-heart sparse MRI framework enables respiratory motion-resolved and easy-to-use free-breathing cardiac whole-heart MRI at temporal resolution and high spatial by the multidimensional compressed sensing (CS) technique. This framework reconstructed 5D whole-heart images including respiratory motion dimensions and separated cardiac without motion correction, which may simplify the MRI workflow and reduce acquisition time (24). For reducing the acquisition time, CS could effectively process high-dimensional images and accelerate image acquisition (2). Prospective gating usually results in low imaging efficiency,

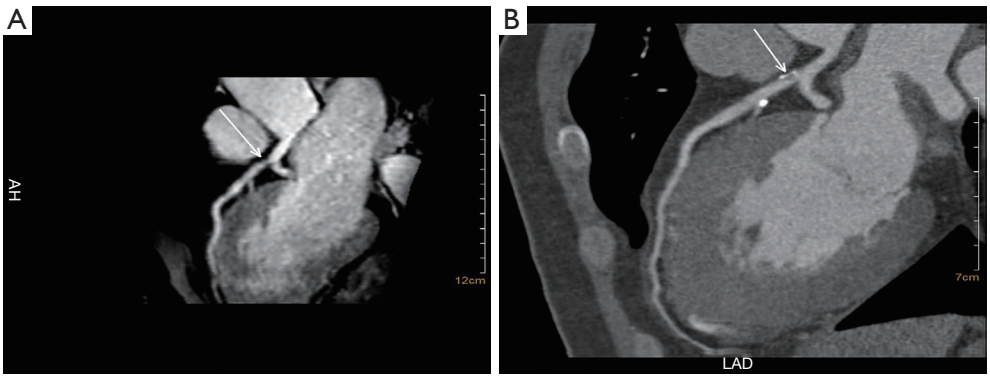

Figure 4 The CPR of 3.0 T whole-heart free-breathing NCE-CMRA based on B-TFE sequence (A) and CCTA (B) from a 40-year-old man. (A) The arrow points to the stenosis of the proximal LAD. (B) The arrow points to the same stenosis of the proximal LAD. CPR, curve planar reformation; NCE-CMRA, non-contrast-enhanced coronary magnetic resonance angiography; B-TFE, balanced turbo-field-echo; CCTA, coronary computed tomography angiography; LAD, left anterior descending; AH, anterior head.

and the imaging time often exceeds 10 minutes, especially in the case of regular respiratory (25). The acquisition time of autonomous breathing navigation with a high acceptance rate could shorten a lot compared with CMRA acquisition of navigation devices. Self-navigating CMRA has been gradually applied in clinical examinations due to its predictable collection time and independence of respiratory patterns (26).

In addition, deep learning reconstruction (DLR) is a forefront topic in recent studies, it has been reported that some techniques such as DLR could improve the contrast noise ratio (CNR) of NCE-CMRA vessels with higher vessel traceability and image quality than traditional CMRA (27-29). DLR technique combined with small golden angle radial sampling could reconstruct short-axis film images more than 5 times faster than traditional methods with higher image quality (30). The deep learning model could rapidly reconstruct undersampling 3D image-based navigators (iNA-VS) for non-rigid motion correction of CMRA, which obviously reduced the reconstruction time compared with traditional reconstruction methods. Meanwhile, the accuracy of non-rigid motion information provided by it was retained (31).

For better visualization, 4D phase-contrast magnetic resonance cardioangiography (4D PC-MRCA) could also improve the visualization of coronary arteries by raising the collection rate of available information during the cardiac impulse (32). In absence of contraindications, sublingual nitroglycerin administration could significantly increase the observable coronary artery diameter and visible vascular length (21). The multi-scale variational neural network (MS-VNN) enabled to quantitative analyze the vessel sharpness of coronary arteries (33).

The clinical application of CCTA to detect significant coronary stenosis and high-risk stratification power with accuracy as high as 95% in patients with low and intermediate-risk factors over the years (34-36). NCE-CMRA can provide an important complement to CCTA without radiation and invasion. As samples with poor image quality had been excluded, there were no significant differences of detecting stenosis among the three vessels in CCTA and NCE-CMRA. This provides an important basis for future clinical applications of NCE-CMRA to detect stenosis.

Limitations

This study was a single-center experiment, all patients had geographical concentration and the relatively small sample population limited generalizability. Due to the need to hold their breath for a long time during the scanning process, some of the patients could not do it, especially the older patients.

The NCE-CMRA data we collected were only relative to CCTA, and the diagnostic difference of coronary artery stenosis between NCE-CMRA and CCTA still needs to be confirmed by ICA. Future prospective studies will address these limitations and will be able to assess the application value of NCE-CMRA in a more comprehensive manner based on clinical results.

Conclusions

The 3.0 T free-breathing whole-heart B-TFE NCE-

CMRA can show the main branches of the coronary arteries with well image quality and reliable visualization during a short acquisition time. It has a good agreement with CCTA for the detection of coronary artery stenosis, which suggests it is expected to be used as a non-invasive and radiation-free option in clinics.

Acknowledgments

This work was supported by the Department of Medical Radiology, Yantai Yuhuangding Hospital, Qingdao University, Department of Cardiology, Yantai Yuhuangding Hospital, Qingdao University, and Weifang Medical College.
Funding: This work was supported by 'Taishan Scholar Project' (grant No. tsqn202103197).

Footnote

Data Sharing Statement: Available at https://cdt.amegroups.com/article/view/10.21037/cdt-22-487/dss

Peer Review File: Available at https://cdt.amegroups.com/article/view/10.21037/cdt-22-487/prf

Conflicts of Interest: All authors have completed the ICMJE uniform disclosure form (available at https://cdt.amegroups.com/article/view/10.21037/cdt-22-487/coif). The authors have no conflicts of interest to declare.

Ethical Statement: The authors are accountable for all aspects of the work in ensuring that questions related to the accuracy or integrity of any part of the work are appropriately investigated and resolved. The study was conducted in accordance with the Declaration of Helsinki (as revised in 2013). The study was approved by the Institutional Review Board of Yantai Yuhuangding Hospital (No. 2021-453). The informed consent was taken from all the patients.

References

1. Saade C, Fakhredin RB, El Achkar B, et al. Coronary Artery Anomalies and Associated Radiologic Findings. J Comput Assist Tomogr 2019;43:572-83.
2. Nakamura M, Kido T, Kido T, et al. Non-contrast compressed sensing whole-heart coronary magnetic resonance angiography at 3T: A comparison with conventional imaging. Eur J Radiol 2018;104:43-8.
3. Di Leo G, Fisci E, Secchi F, et al. Diagnostic accuracy of magnetic resonance angiography for detection of coronary artery disease: a systematic review and meta-analysis. Eur Radiol 2016;26:3706-18.
4. Edvardsen T, Asch FM, Davidson B, et al. Non-invasive imaging in coronary syndromes: recommendations of the European Association of Cardiovascular Imaging and the American Society of Echocardiography, in collaboration with the American Society of Nuclear Cardiology, Society of Cardiovascular Computed Tomography, and Society for Cardiovascular Magnetic Resonance. Eur Heart J Cardiovasc Imaging 2022;23:e6-e33.
5. Lee SE, Sung JM, Rizvi A, et al. Quantification of Coronary Atherosclerosis in the Assessment of Coronary Artery Disease. Circ Cardiovasc Imaging 2018;11:e007562.
6. Kato Y, Ambale-Venkatesh B, Kassai Y, et al. Non-contrast coronary magnetic resonance angiography: current frontiers and future horizons. MAGMA 2020;33:591-612.
7. Tian D, Zhao SH, Wang Y, et al. Unenhanced Whole-Heart Coronary MRA: Prospective Intraindividual Comparison of 1.5-T SSFP and 3-T Dixon Water-Fat Separation GRE Methods Using Coronary Angiography as Reference. AJR Am J Roentgenol 2022;219:199-211.
8. Weiss KJ, Eggers H, Stehning C, et al. Feasibility and Robustness of 3T Magnetic Resonance Angiography Using Modified Dixon Fat Suppression in Patients With Known or Suspected Peripheral Artery Disease. Front Cardiovasc Med 2020;7:549392.
9. Zhang L, Song X, Dong L, et al. Additive value of 3T cardiovascular magnetic resonance coronary angiography for detecting coronary artery disease. J Cardiovasc Magn Reson 2018;20:29.
10. Bratis K, Henningsson M, Grigoratos C, et al. 'Image-navigated 3-dimensional late gadolinium enhancement cardiovascular magnetic resonance imaging: feasibility and initial clinical results'. J Cardiovasc Magn Reson 2017;19:97.
11. Sun Z, Zhang Q, Zhao H, et al. Retrospective assessment of at-risk myocardium in reperfused acute myocardial

infarction patients using contrast-enhanced balanced steady-state free-precession cardiovascular magnetic resonance at 3T with SPECT validation. J Cardiovasc Magn Reson 2021;23:25.
12. Kawada H, Goshima S, Sakurai K, et al. Utility of Noncontrast Magnetic Resonance Angiography for Aneurysm Follow-Up and Detection of Endoleaks after Endovascular Aortic Repair. Korean J Radiol 2021;22:513-24.
13. Zahergivar A, Kocher M, Waltz J, et al. The diagnostic value of non-contrast magnetic resonance coronary angiography in the assessment of coronary artery disease: A systematic review and meta-analysis. Heliyon 2021;7:e06386.
14. Nazir MS, Bustin A, Hajhosseiny R, et al. High-resolution non-contrast free-breathing coronary cardiovascular magnetic resonance angiography for detection of coronary artery disease: validation against invasive coronary angiography. J Cardiovasc Magn Reson 2022;24:26.
15. Velasco Forte MN, Valverde I, Prabhu N, et al. Visualization of coronary arteries in paediatric patients using whole-heart coronary magnetic resonance angiography: comparison of image-navigation and the standard approach for respiratory motion compensation. J Cardiovasc Magn Reson 2019;21:13.
16. Kumar SP, Phadke KV, Vydrová J, et al. Visual and Automatic Evaluation of Vocal Fold Mucosal Waves Through Sharpness of Lateral Peaks in High-Speed Videokymographic Images. J Voice 2020;34:170-8.
17. Sun B, Chen Z, Duan Q, et al. A direct comparison of 3 T contrast-enhanced whole-heart coronary cardiovascular magnetic resonance angiography to dual-source computed tomography angiography for detection of coronary artery stenosis: a single-center experience. J Cardiovasc Magn Reson 2020;22:40.
18. Becker H, Wattenberg M, Barth P, et al. Impact of different respiratory monitoring techniques on respiration-dependent stroke-volume measurements assessed by real-time magnetic resonance imaging. Z Med Phys 2019;29:349-58.
19. Hajhosseiny R, Bustin A, Munoz C, et al. Coronary Magnetic Resonance Angiography: Technical Innovations Leading Us to the Promised Land? JACC Cardiovasc Imaging 2020;13:2653-72.
20. Hirai K, Kido T, Kido T, et al. Feasibility of contrast-enhanced coronary artery magnetic resonance angiography using compressed sensing. J Cardiovasc Magn Reson 2020;22:15.
21. Heer T, Reiter S, Trißler M, et al. Effect of Nitroglycerin on the Performance of MR Coronary Angiography. J Magn Reson Imaging 2017;45:1419-28.
22. Pang J, Sharif B, Fan Z, et al. ECG and navigator-free four-dimensional whole-heart coronary MRA for simultaneous visualization of cardiac anatomy and function. Magn Reson Med 2014;72:1208-17.
23. Kim SJ, Choi CG, Kim JK, et al. Effects of MR parameter changes on the quantification of diffusion anisotropy and apparent diffusion coefficient in diffusion tensor imaging: evaluation using a diffusional anisotropic phantom. Korean J Radiol 2015;16:297-303.
24. Feng L, Coppo S, Piccini D, et al. 5D whole-heart sparse MRI. Magn Reson Med 2018;79:826-38.
25. Lu H, Guo J, Zhao S, et al. Assessment of Non-contrast-enhanced Dixon Water-fat Separation Compressed Sensing Whole-heart Coronary MR Angiography at 3.0 T: A Single-center Experience. Acad Radiol 2022;29 Suppl 4:S82-90.
26. Piccini D, Bonanno G, Ginami G, et al. Is there an optimal respiratory reference position for self-navigated whole-heart coronary MR angiography? J Magn Reson Imaging 2016;43:426-33.
27. Yokota Y, Takeda C, Kidoh M, et al. Effects of Deep Learning Reconstruction Technique in High-Resolution Non-contrast Magnetic Resonance Coronary Angiography at a 3-Tesla Machine. Can Assoc Radiol J 2021;72:120-7.
28. Küstner T, Munoz C, Psenicny A, et al. Deep-learning based super-resolution for 3D isotropic coronary MR angiography in less than a minute. Magn Reson Med 2021;86:2837-52.
29. Qi H, Fuin N, Cruz G, et al. Non-Rigid Respiratory Motion Estimation of Whole-Heart Coronary MR Images Using Unsupervised Deep Learning. IEEE Trans Med Imaging 2021;40:444-54.
30. Hauptmann A, Arridge S, Lucka F, et al. Real-time cardiovascular MR with spatio-temporal artifact suppression using deep learning-proof of concept in congenital heart disease. Magn Reson Med 2019;81:1143-56.
31. Malavé MO, Baron CA, Koundinyan SP, et al. Reconstruction of undersampled 3D non-Cartesian image-based navigators for coronary MRA using an unrolled deep learning model. Magn Reson Med 2020;84:800-12.
32. Bustamante M, Gupta V, Carlhäll CJ, et al. Improving visualization of 4D flow cardiovascular magnetic resonance with four-dimensional angiographic data: generation of a 4D phase-contrast magnetic resonance CardioAngiography (4D PC-MRCA). J Cardiovasc Magn Reson 2017;19:47.

33. Fuin N, Bustin A, Küstner T, et al. A multi-scale variational neural network for accelerating motion-compensated whole-heart 3D coronary MR angiography. Magn Reson Imaging 2020;70:155-67.
34. Linde JJ, Kelbæk H, Hansen TF, et al. Coronary CT Angiography in Patients With Non-ST-Segment Elevation Acute Coronary Syndrome. J Am Coll Cardiol 2020;75:453-63.
35. Lin A, Manral N, McElhinney P, et al. Deep learning-enabled coronary CT angiography for plaque and stenosis quantification and cardiac risk prediction: an international multicentre study. Lancet Digit Health 2022;4:e256-65.
36. Schuijf JD, Matheson MB, Ostovaneh MR, et al. Ischemia and No Obstructive Stenosis (INOCA) at CT Angiography, CT Myocardial Perfusion, Invasive Coronary Angiography, and SPECT: The CORE320 Study. Radiology 2020;294:61-73.

Cite this article as: Chen Y, Guo H, Dong P, Li Y, Zhang Z, Mao N, Chu T, Sun Z, Wang F, Feng Z, Wang H, Ma H. Feasibility of 3.0 T balanced fast field echo non-contrast-enhanced whole-heart coronary magnetic resonance angiography. Cardiovasc Diagn Ther 2023;13(1):51-60. doi: 10.21037/cdt-22-487